Saudi Pharmaceutical Journal 28 (2020) 1172–1181

Contents lists available at ScienceDirect

Saudi Pharmaceutical Journal

journal homepage: www.sciencedirect.com

Original article

Prenylated phenolics as promising candidates for combination antibacterial therapy: Morusin and kuwanon G

Petruta Aelenei [a,b], Cristina Mihaela Rimbu [c], Cristina Elena Horhogea [c,*], Andrei Lobiuc [d,e], Anca-Narcisa Neagu [f], Simona Isabela Dunca [f], Iuliana Motrescu [g], Gabriel Dimitriu [h], Ana Clara Aprotosoaie [a], Anca Miron [a]

[a] Department of Pharmacognosy, Faculty of Pharmacy, Grigore T. Popa University of Medicine and Pharmacy Iasi, Universitatii Str. 16, Iasi 700115, Romania
[b] Regulatory Affairs Department, Fiterman Pharma LLC, Pacurari Road 127, Iasi 700544, Romania
[c] Department of Public Health, Faculty of Veterinary Medicine, Ion Ionescu de la Brad University of Agricultural Sciences and Veterinary Medicine of Iasi, Mihail Sadoveanu Al. 8, Iasi 700489, Romania
[d] Human Health and Development Department, Stefan cel Mare University of Suceava, Universitatii Str. 13, Suceava 720229, Romania
[e] Integrated Research Centre for Environmental Studies in the N-E Area - CERNESIM, L2 Laboratory, Alexandru Ioan Cuza University of Iasi, Carol I Bd. 20A, Iasi 700506, Romania
[f] Faculty of Biology, Alexandru Ioan Cuza University of Iasi, Carol I Bd. 20A, Iasi 700505, Romania
[g] Science Department & Research Institute for Agriculture and Environment, Ion Ionescu de la Brad University of Agricultural Sciences and Veterinary Medicine of Iasi, Mihail Sadoveanu Al. 3, Iasi 700490, Romania
[h] Department of Medical Informatics and Biostatistics, Faculty of Medicine, Grigore T. Popa University of Medicine and Pharmacy Iasi, Universitatii Str. 16, Iasi 700115, Romania

ARTICLE INFO

Article history:
Received 1 June 2020
Accepted 11 August 2020
Available online 18 August 2020

Keywords:
Morusin
Kuwanon G
Antibiotics
Antibacterial synergy
MRSA
Membrane permeabilization

ABSTRACT

Combination of antibiotics with natural products is a promising strategy for potentiating antibiotic activity and overcoming antibiotic resistance. The purpose of the present study was to investigate whether morusin and kuwanon G, prenylated phenolics in *Morus* species, have the ability to enhance antibiotic activity and reverse antibiotic resistance in *Staphylococcus aureus* and *Staphylococcus epidermidis*. Commonly used antibiotics (oxacillin, erythromycin, gentamicin, ciprofloxacin, tetracycline, clindamycin) were selected for the combination studies. Checkerboard and time-kill assays were used to investigate potential bacteriostatic and bactericidal synergistic interactions, respectively between morusin or kuwanon G and antibiotics. According to both fractional inhibitory concentration index and response surface models, twenty combinations (14 morusin-antibiotic combinations, six kuwanon G-antibiotic combinations) displaying bacteriostatic synergy were identified, with 4–512-fold reduction in the minimum inhibitory concentration values of antibiotics in combination. Both morusin and kuwanon G reversed oxacillin resistance of methicillin-resistant *Staphylococcus aureus.* In addition, morusin reversed tetracycline resistance of *Staphylococcus epidermidis*. At half of the minimum inhibitory concentrations, combinations of morusin with oxacillin or gentamicin showed bactericidal synergy against methicillin-resistant *Staphylococcus aureus.* Fluorescence and differential interference contrast microscopy and scanning electron microscopy showed an increase in the membrane permeability and massive leakage of cellular content in methicillin-resistant *Staphylococcus aureus* exposed to morusin or kuwanon G. Overall, our findings strongly indicate that both prenylated compounds are good candidates for the development of novel antibacterial combination therapies.

1. Introduction

Despite significant advances in anti-infective therapy, infectious diseases are still a main cause of morbidity and mortality worldwide. Inappropriate prescribing and overuse of antibiotics led to the emergence of antibiotic resistance (single- and multi-drug resistance), a contributing factor to the high mortality rate of infectious diseases (Lee Ventola, 2015; Zacchino et al., 2017). Carbapenem-resistant *Acinetobacter baumannii* and *Pseudomonas*

* Corresponding author.
E-mail addresses: cristinae.horhogea@gmail.com, chorhogea@uaiasi.ro (C.E. Horhogea).
Peer review under responsibility of King Saud University.

Production and hosting by Elsevier

https://doi.org/10.1016/j.jsps.2020.08.006
1319-0164/

aeruginosa, carbapenem-resistant and extended spectrum beta-lactamase producing Enterobacteriaceae, methicillin-resistant *Staphylococcus aureus* (MRSA), vancomycin-resistant *Enterococcus faecium*, fluoroquinolone-resistant *Campylobacter* spp., clarithromycin-resistant *Helicobacter pylori* are priority drug-resistant pathogens that represent a major health issue nowadays (Subramani et al., 2017). In addition, the development of new antibiotics significantly decreased in the past 30 years, only six new antibiotics being developed and approved in 2010–2014 (Lee Ventola, 2015). In these circumstances, combination antibiotic therapy has been used in clinical practice to restore the efficacy of antibiotics. Unfortunately, in some cases, it did not give the expected results (Zacchino et al., 2017). A promising alternative seems to be the combination of antibiotics with low molecular weight plant metabolites. Such combinations displaying synergistic effects are of great therapeutic interest (Aelenei et al., 2016; Zacchino et al., 2017).

Among low molecular weight plant metabolites, prenylated phenolics showed not only potent antibacterial activity but also promising antibiotic-potentiating effects. For example, a farnesylated salicylic acid derivative from the leaves of *Piper multiplinervium* C. DC. had excellent activity against both Gram-positive (*S. aureus, Mycobacterium smegmatis*) and Gram-negative bacteria (*Escherichia coli*, *Klebsiella pneumoniae, P. aeruginosa*) but also *Candida albicans* with minimum inhibitory concentration (MIC) values between 2.5 and 5 μg/mL (Rüegg et al., 2006). Eryvarin W, a double prenylated pterocarpene from the roots of *Erythrina variegata* L., showed MICs of 1.56–3.13 μg/mL against MRSA strains, which lie in the range of the MIC values of vancomycin (MICs = 0.78 – 3.13 μg/mL) (Tanaka et al., 2011). 7,9,2′,4′-Tetrahydroxy-8-isopentenyl-5-methoxychalcone, a prenylated chalcone from the roots of *Sophora flavescens* Ait., demonstrated excellent activity against MRSA and vancomycin-resistant enterococci (VRE) with MICs ranging from 1 to 8 μg/mL; in addition, the chalcone acted synergistically with ampicillin and gentamicin against MRSA and VRE (Lee et al., 2010). α-Mangostin, a prenylated xanthone from *Garcinia mangostana* L. stem bark, inhibited the growth of VRE and MRSA (MIC = 6.25 and 6.25 – 12.5 μg/mL, respectively); moreover, it potentiated the activity of gentamicin and vancomycin against VRE and MRSA, respectively (synergistic interactions) (Sakagami et al., 2005). Another *Garcinia* prenylated xanthone, γ-mangostin, acted synergistically with penicillin G against pathogenic *Leptospira interrogans* (Seesom et al., 2013). 5-*O*-Methylglovanon, a prenylated flavanone isolated from *Glycosmis* plants, inhibited the growth of ampicillin resistant *S. aureus* and *Staphylococcus epidermidis* isolates with MICs ranging from 12.5 to 50 μg/mL and showed synergy with ampicillin against same isolates (Zhou et al., 2011). Xanthohumol, a prenylated chalcone in hop (*Humulus lupulus* L.), was found to synergize with several antibiotics (ciprofloxacin, gentamicin, oxacillin, rifampicin) against MRSA isolate while its desmethyl derivative was synergistic only with ciprofloxacin and gentamicin (Bocquet et al., 2019).

Morusin and kuwanon G (Fig. 1) are prenylated phenolics in *Morus* species (Abbas et al., 2014; Gao et al., 2017; Guo et al., 2016). *Morus* species (mulberry, Moraceae) are crop trees widely cultivated for the leaves representing the only natural feed available for silkworms (*Bombyx mori* L.). In addition, mulberry root and stem barks, leaves and fruits have been used in traditional medicine for the prevention and treatment of numerous disorders (Turan et al., 2017; Vijayan et al., 2011). Biologically active phytochemicals belonging to different classes (flavonoids, benzofurans, alkaloids) have been isolated from *Morus* species (Hosseini et al., 2018; Zhang et al., 2018). Morusin (prenylflavone) was reported to possess antioxidant, anti-inflammatory and antitumor activities (Gao et al., 2017) whereas kuwanon G (Diels – Alder type adduct) was found to exhibit antioxidant, anti-inflammatory, immunomodulatory and anti-*Ichthyophthirius multifiliis* (agent of ichthyophthiriasis) activities (Guo et al., 2016; Nasir et al., 2017). The up-to-date studies on the antibacterial activity of morusin and kuwanon G focused on susceptibility tests and less on interactions with antibiotics (Mazimba et al., 2011; Pang et al., 2019; Park et al., 2003; Sohn et al., 2004; Wu et al., 2019; Zuo et al., 2018). Accordingly, the aim of the present work was to assess the interactions between these two prenylated compounds and antibiotics to find combinations with more efficient antibacterial effects against *S. aureus* and *S. epidermidis*.

2. Material and methods

2.1. Bacterial strains and culture media

S. aureus ATCC 43300 (MRSA) and *S. epidermidis* ATCC 12228 were purchased from the American Type Culture Collection. Methicillin-susceptible *S. aureus* ATCC 6538 (MSSA) was provided by the Public Health Department of the Faculty of Veterinary

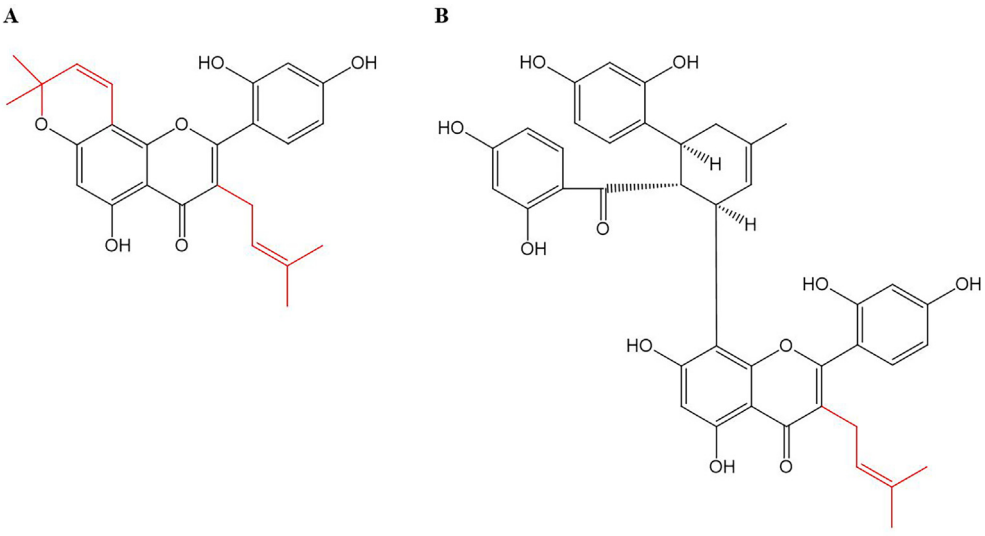

Fig. 1. Structures of morusin (A) and kuwanon G (B).

Medicine, Ion Ionescu de la Brad University of Agricultural Sciences and Veterinary Medicine of Iasi (Romania). Mueller-Hinton broth and Mueller-Hinton agar were purchased from Oxoid (Basingstoke, UK).

2.2. Antibacterial agents

Oxacillin sodium monohydrate, erythromycin (base), gentamicin sulfate, ciprofloxacin hydrochloride, tetracycline hydrochloride and clindamycin phosphate were purchased from Sigma-Aldrich (Steinheim, Germany). Morusin and kuwanon G (purity min. 97%) were obtained from Carbosynth Limited (Berkshire, UK).

2.3. Chemicals

Acridine orange, dibasic potassium phosphate, dimethyl sulfoxide (DMSO), disodium hydrogen phosphate, ethanol 99.8%, glutaraldehyde solution grade I 50%, propidium iodide, propylene oxide and osmium tetroxide were purchased from Sigma-Aldrich (Steinheim, Germany).

2.4. Susceptibility tests

MIC values were determined by the broth microdilution method according to the Clinical & Laboratory Standards Institute guidelines (CLSI, 2017) and previous reports (Aelenei et al., 2019a; Hendry et al., 2009; Segatore et al., 2012) with slight modifications. Briefly, the bacterial inoculum (1.5×10^8 CFU/mL) was incubated with serial two-fold dilutions of antibacterial agent (5120 – 0.156 μg/mL for antibiotics and 1000 – 2 μg/mL for morusin and kuwanon G) for 20 h at 37 °C. The bacterial growth was recorded spectrophotometrically at 600 nm using a microplate reader Stat Fax 3200 (Awareness Technology, Palm City, Florida, USA). The percentage of bacterial growth in each well was calculated as follows: $[(OD_{\text{antibacterial agent well}} - OD_{\text{background}}) / (OD_{\text{antibacterial agent free well}} - OD_{\text{background}})] \times 100$, where OD stands for optical density; the background was the growth medium without any bacteria inoculated. MIC was the lowest concentration of antibacterial agent causing bacterial growth inhibition $\geq$ 90% in comparison with the antibacterial agent-free control (positive control) (Chan et al., 2013) and it was determined as the median of three independent experiments (Segatore et al., 2012).

2.5. Assessment of MRSA membrane integrity

The effects of morusin and kuwanon G on the integrity of MRSA ATCC 43300 membrane were evaluated by the fluorescence and differential interference contrast microscopy according to Aquino et al. (2010) with slight modifications. The exponential-phase cell suspension of MRSA ATCC 43300 was washed two times with phosphate buffered saline (PBS) (pH = 7.2) (Araya-Cloutier et al., 2018) and further subjected to incubation at 37 °C with prenylated compounds (at 2 × MIC) or DMSO (control). Aliquots (1 mL) were taken at 15, 30, 60, 120 and 180 min, stained with 3 μL of 1:1 mixture of 20 mM propidium iodide and 0.01% acridine orange, vortexed and incubated in dark at 37 °C for 15 min. Propidium iodide and acridine orange were removed by centrifugation with further resuspension of the sediment in 1 mL PBS. Samples were analyzed with Leica Confocal Laser Scanning Microscope (TCS SPE DM 5500Q) using the I3 blue excitation range filter cube (BP 450 – 490 nm band pass filter) and the N2.1 green excitation filter cube (BP 515 – 560 nm band pass filter). At least five independent images per sample were captured. For each image, the ratio (%) between the red fluorescent cells and total cells visualized with differential interference contrast was calculated.

2.6. Assessment of MRSA membrane morphology

In order to investigate the effects of morusin and kuwanon G on the morphology of MRSA ATCC 43300 membrane, scanning electron microscopy (SEM) was performed according to Basri et al. (2013) with slight modifications. After 24 h incubation at 37 °C with morusin or kuwanon G (each at ½ × MIC), the treated and untreated (control) bacterial cell suspensions were centrifuged at 2000 rpm for 10 min, washed two times with 0.1 M PBS (pH = 7.2), fixed with 2.5% glutaraldehyde in 0.1 M PBS at 4 °C for 2 h, washed with PBS twice and post-fixed with 1% osmium tetroxide in sterile water at room temperature for 4 h. The bacterial cells were further washed two times with PBS, successively dehydrated with a series of ethanol dilutions (30%, 50%, 70% and 99.8%, 15 min for each dilution) and finally suspended in propylene oxide overnight. For imaging the samples, FEI Quanta 450 Scanning Electron Microscope was used (high vacuum mode (about 10–4 Pa), electron acceleration voltage of 12.5 V).

2.7. Checkerboard assay

The two-dimensional checkerboard microdilution assay was used to investigate the interactions between morusin/kuwanon G and antibiotics according to previously described protocols (Aelenei et al., 2019a; Hendry et al., 2009) with minor changes. In brief, in sterile 96-well microtiter plates containing Mueller-Hinton broth, the antibiotic (20 μL) was serially diluted horizontally while the prenylated compound (10 μL) was serially diluted vertically. Then, each well was inoculated with the bacterial suspension (1.5×10^8 CFU/mL, 30 μL), the final volume in each well being 200 μL. The concentrations of antibacterial agents (antibiotic or prenylated compound) in the wells varied from 4 × MIC to 1/512 × MIC. Positive (bacterial inoculum and Mueller-Hinton broth) and negative (prenylated compound or antibiotic and Mueller-Hinton broth) control wells were also prepared. The data analysis was performed using the fractional inhibitory concentration index (FICI) (Mulyaningsih et al., 2010; Zuo et al., 2018), isobolograms (van Vuuren and Viljoen, 2011) and response surface approach using the ΔE model (Segatore et al., 2012). The FICI model is based on Loewe additivity theory whereas the ΔE model bases on Bliss independence theory (Meletiadis et al., 2005; Segatore et al., 2012). FICI was calculated for the first wells without bacterial growth neighboring the wells with bacterial growth as follows: $FICI = FIC_{\text{antibiotic}} + FIC_{\text{prenylated compound}} = MIC_{\text{antibiotic in combination}} / MIC_{\text{antibiotic alone}} + MIC_{\text{prenylated compound in combination}} / MIC_{\text{prenylated compound alone}}$ (Otto et al., 2019; Zuo et al., 2018). The type of interaction between morusin/kuwanon G and antibiotics was defined on the basis of FICI value: synergy (the final effect greater than the sum of the individual effects) when FICI $\leq$ 0.5, addition (the final effect equal to the sum of the individual effects) when 0.5 < FICI $\leq$ 1.0, indifference (no interaction) when 1.0 < FICI $\leq$ 4, antagonism (the final effect less than the sum of the individual effects) when FICI > 4 (Bassolé and Juliani, 2012; Mulyaningsih et al., 2010; van Vuuren and Viljoen, 2011). In isobolograms (graphs representing the combination effects), the ratio points falling below the 0.5 : 0.5, 1 : 1 and 4 : 4 lines indicate synergy, addition and indifference, respectively whereas those falling above the 4 : 4 line express antagonism (Caesar and Cech, 2019; van Vuuren and Viljoen, 2011). In the response surface approach, the type of interaction is defined by the difference (ΔE) between the predicted ($E_{\text{predicted}}$) and measured (E_{measured}) percentages of bacterial growth, with $E_{\text{predicted}}$ being the product of the experimental percentages of bacterial growth for each component of the combination when acting alone ($E_{\text{predicted}} = E_{\text{component 1 alone}} \times E_{\text{component 2 alone}}$). $E_{\text{predicted}}$ was calculated for all the combinations tested experimentally. The concentrations of the two antibacterial agents

and ΔE values were further plotted three-dimensionally, with synergy and antagonism being expressed by the points of the response surface (ΔE) above and below zero, respectively. To characterize the whole interaction surface, the sum of all statistically significant synergistic (ΣSYN) and antagonistic (ΣANT) interactions were calculated; values lower than 100%, between 100% and 200% and higher than 200% indicate weak, moderate and strong interactions, respectively (Meletiadis et al., 2005; Segatore et al., 2012).

2.8. Time-kill assay

Time-kill experiments were performed according to a previously described method (Mulyaningsih et al., 2010) with minor changes. The prenylated compounds and antibiotics were tested alone and in combination at sub-inhibitory concentrations (½ × MIC). Briefly, the antibacterial agent alone/combination (0.11 mL of prenylated compound and/or 0.22 mL of antibiotic in concentrations to provide ½ × MIC), bacterial inoculum (1.5×10^8 CFU/mL, 0.33 mL) and Mueller-Hinton broth (up to 2.2 mL) were added into screw-capped tubes. Positive controls containing only Mueller-Hinton broth and bacterial suspension were also prepared. After 0, 4, 24 and 48 h of incubation at 37 °C, 120 μL were removed from each tube and diluted with physiological saline solution to a volume of 1 mL from which aliquots of 100 μL were further withdrawn and spread on Mueller-Hinton agar plates. The bacterial colonies (CFU/mL) were counted after 24 h incubation at 37 °C and the difference in bacterial killing ($\triangle LC_{24}$) induced by the combination in comparison with its most active component tested alone, expressed as $\log_{10}$ CFU/mL, was calculated. An interaction is described as synergistic if $\triangle LC_{24} \geq 2$ $\log_{10}$ CFU/mL, additive if $\triangle LC_{24}$ = 1–2 $\log_{10}$ CFU/mL, indifferent if $\triangle LC_{24} = \pm 1$ $\log_{10}$ CFU/mL and antagonistic if $\triangle LC_{24} > -1$ $\log_{10}$ CFU/mL (Zuo et al., 2016). Killing curves were also plotted. The experiments were performed at least thrice and the results were expressed as mean ± standard deviation.

2.9. Statistical analysis

All experiments were done in biological triplicates. Statistical analyses were performed using analysis of variance (ANOVA) (SPSS software package 18.0).

3. Results and discussion

In our search for phytochemicals that could increase antibiotic efficacy, we investigated the interactions between morusin or kuwanon G and six conventional antibiotics (oxacillin, erythromycin, gentamicin, ciprofloxacin, tetracycline, clindamycin) against *S. aureus* (MSSA and MRSA) and S. *epidermidis*. Both *Staphylococcus* species are nosocomial pathogens causing severe infections (Zhou et al., 2011). Moreover, the emergence of drug resistance significantly limited the therapeutic options and made staphylococcal infections difficult to treat. In case of MRSA infections, antibiotic monotherapy (vancomycin, teicoplanin, telavancin, daptomycin, ceftaroline, linezolid) and antibiotic combination therapy (vancomycin and beta-lactams, ceftaroline and daptomycin) have limitations with respect to tolerance, side effects, costs, development of resistance and cross-resistance (Choo and Chambers, 2016). Same limitations arise in the treatment of the infections caused by resistant *S. epidermidis*, common in broken-skinned, immunocompromised and implanted patients (Eladli et al., 2019; Otto, 2009). Therefore, combinations of antibiotics with natural products, exhibiting synergistic interactions, represent a promising strategy to achieve increased efficacy and reduced side effects (Zhou et al., 2011).

3.1. Antibacterial activity of morusin and kuwanon G

Determination of MIC values is a mandatory step in the assessment of interactions between antibacterial agents in combination. Accordingly, morusin and kuwanon G were firstly tested alone against MSSA ATCC 6538, MRSA ATCC 43300 and *S. epidermidis* ATCC 12228. Both prenylated compounds showed very good antibacterial activity against tested strains, including MRSA, with MIC values of 6.25 and 12.50 μg/mL, respectively. Natural compounds are considered to have very good, good, moderate and low antibacterial activities if their MICs ≤ 15 μg/mL, 15 < MICs ≤ 25 μg/mL, 25 < MICs ≤ 100 μg/mL and MICs > 100 μg/mL, respectively (Araya-Cloutier, 2017). It is worth mentioning that our previous investigations on morusin and kuwanon G found irrelevant antibacterial effects against Gram-negative bacteria (*E. coli*, *P. aeruginosa*) (data not shown). With respect to morusin, our results are in agreement with previous studies reporting very good and good antibacterial effects against MSSA and *S. epidermidis* (MIC = 6.30 – 25 and 20 μg/mL, respectively) but moderate and low activity against Gram-negative bacteria (MIC = 62.5 μg/mL against *P. aeruginosa,* MIC > 100 μg/mL against *E. coli*) (Mazimba et al., 2011; Pang et al., 2019; Sohn et al., 2004; Wu et al., 2019; Zuo et al., 2018). Zuo et al. (2018) have recently reported very good to moderate antibacterial effects for morusin against clinical MRSA isolates (MIC = 8 – 32 μg/mL). Referring to kuwanon G, recent studies reported very good antibacterial activity against MSSA and MRSA isolates (MICs of 2 and 8 μg/mL) (Wu et al., 2019).

Prenylation is undoubtedly the major contributor to the antibacterial potency of morusin and kuwanon G. Prenylation increases the hydrophobicity of the molecule resulting in an increased affinity for the bacterial cytoplasmic membrane with disturbance of its organization and biophysical properties (Wesołowska et al., 2014). Being highly lipophilic due to the prenyl moiety, prenylated compounds hardly penetrate the lipopolysaccharide layer of the outer membrane of Gram-negative bacteria (Araya-Cloutier, 2017). This explains, at least in part, the irrelevant activity of prenylated compounds against Gram-negative bacteria.

3.2. Effects on the integrity and morphology of MRSA membrane

In an attempt to elucidate the mechanisms underlying their antibacterial potential, morusin and kuwanon G have been recently investigated with respect to their effects on MSSA membrane; both compounds were found to disrupt the bacterial membrane (Pang et al., 2019; Wu et al., 2019). In the present study, we examined their effects on the integrity and morphology of MRSA (*S. aureus* ATCC 43300) membrane using the fluorescence and differential interference contrast microscopy and SEM, respectively. Substantial alterations in the membrane permeability were observed in MRSA exposed to morusin or kuwanon G.

In the fluorescence and differential interference contrast microscopy studies, two fluorescent DNA-binding dyes were used: acridine orange (green fluorescence) that crosses the membranes of both viable (intact membrane) and dead (leaky membrane) cells and propidium iodide (red fluorescence) that does not permeate the viable cell membranes (Kirchhoff and Cypionka, 2017) but permeates the dead cells. The fluorescence and differential interference contrast microscopy images (Fig. 2A,B,C and Fig. S1A,B,C respectively) show that both morusin and kuwanon G (each at 2 × MIC) increased the permeability of MRSA ATCC 43300 membrane. MRSA ATCC 43300 exposed to morusin or kuwanon G had propidium iodide fluorescence (red) indicating loss of bacterial membrane integrity. The control had acridine orange fluorescence (green) indicating undamaged bacterial membrane throughout the entire exposure period. The increase in membrane permeability

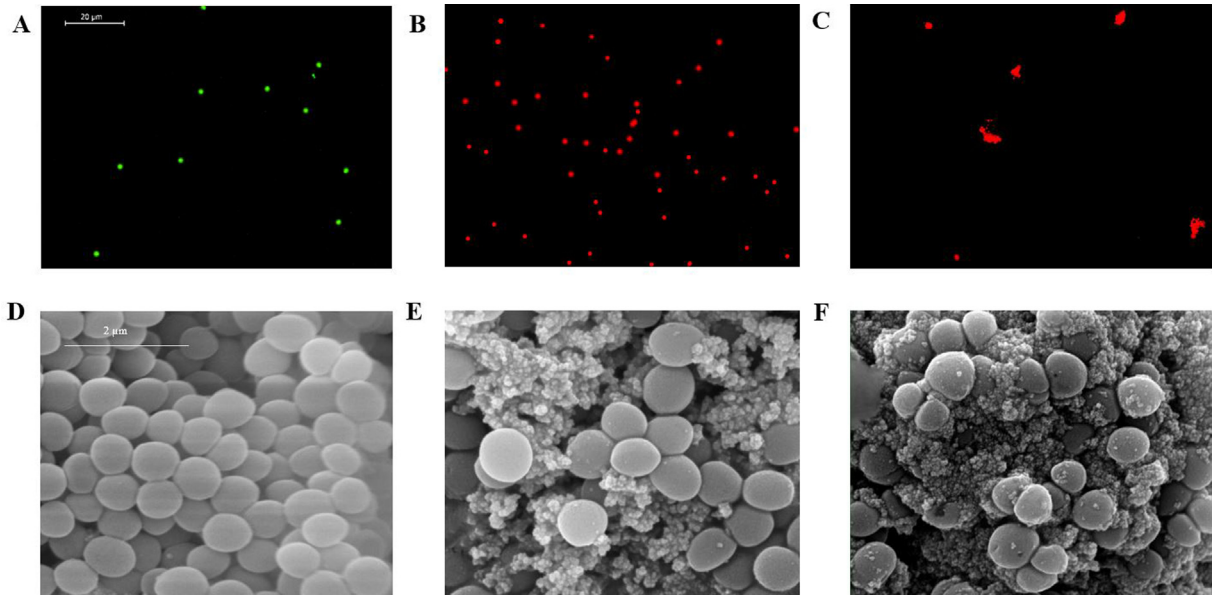

Fig. 2. Effects of exposure to morusin and kuwanon G on the integrity (A, B, C) and morphology (D, E, F) of *S. aureus* ATCC 43300 (MRSA) membrane. Fluorescence images of *S. aureus* ATCC 43300 (MRSA) after 60 min exposure to DMSO (control) (A), morusin (2 × MIC) (B) and kuwanon G (2 × MIC) (C). Scanning electron microscopy (SEM) of *S. aureus* ATCC 43300 (MRSA) after 24 h incubation: no treatment (D), treated with morusin (½ × MIC) (E) and kuwanon G (½ × MIC) (F).

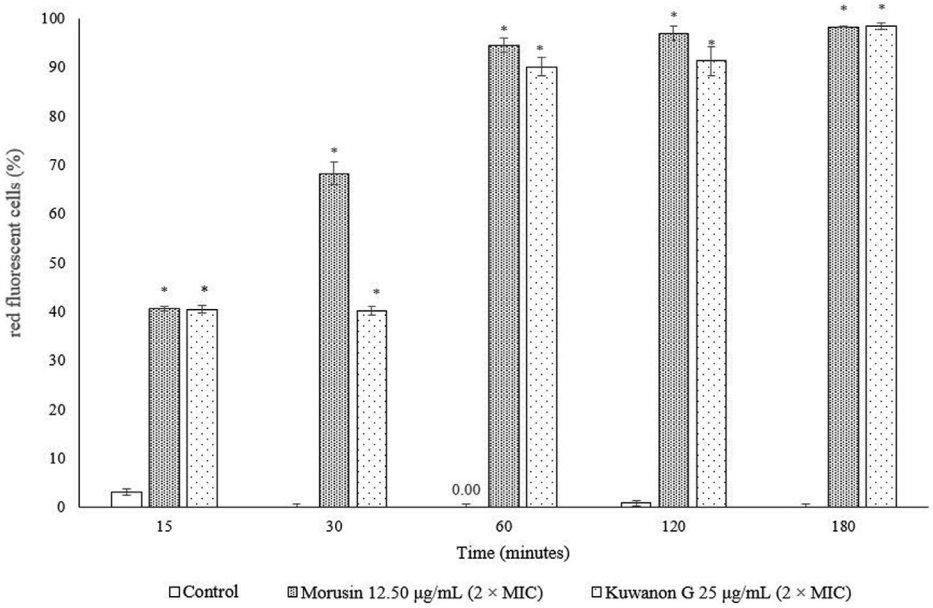

Fig. 3. Effects of exposure to morusin (2 × MIC) and kuwanon G (2 × MIC) on membrane permeability of exponential-phase cultures of *S. aureus* ATCC 43300 (MRSA) expressed as the percentage of red fluorescent cells in the population. Each bar represents the mean acquired by counting the captured cells and the error bars represent the standard deviations. *p < 0.05 *vs.* control (ANOVA).

was time-dependent. Morusin and kuwanon G caused red fluorescence in about 40% bacterial cells after only 15 min exposure. Higher percentages of red fluorescence cells (> 90%) were recorded after 60 min exposure to morusin or kuwanon G (Fig. 3).

The effects of morusin and kuwanon G (each at ½ × MIC) on the morphology of MRSA ATCC 43300 membrane were assessed by SEM. Untreated MRSA showed normal morphology with spherical, regular and smooth surface grape-like clusters whereas massive leakage of cellular content was observed in MRSA treated with morusin or kuwanon G (Fig. 2D,E,F).

3.3. Interactions of morusin and kuwanon G with antibiotics

The effects of morusin and kuwanon G in combination with antibiotics were further evaluated using the checkerboard assay. The antibiotics selected for the interaction studies (oxacillin, erythromycin, gentamicin, ciprofloxacin, tetracycline and clindamycin) are commonly used, belong to different classes (beta-lactams, macrolides, aminoglycosides, quinolones, tetracyclines and lincosamides, respectively) and have different mechanisms of activity (oxacillin: inhibition of cell wall biosynthesis, ciprofloxa-

cin: inhibition of DNA replication, erythromycin, gentamicin, tetracycline, clindamycin: inhibition of protein synthesis) (Kohanski et al., 2010; Segatore et al., 2012). Unfortunately, they can develop severe side effects (oxacillin: interstitial nephritis, drug-induced hepatitis; erythromycin: ototoxicity, cardiac side effects; gentamicin: ototoxicity, nephrotoxicity; ciprofloxacin: seizures, tendinitis, tendon rupture; tetracycline: photosensitivity; clindamycin: diarrhea, maculopapular rash) (Alikhani & Salehifar, 2012; Cunha, 2001; Lee et al., 2008). Therefore, their use in combination with natural products having antibiotic potentiating effects would allow the reduction of antibiotic doses in combination and consequently, minimization of antibiotic side effects.

As mentioned in 2.7., the interactions in combination were assessed using the FICI model, isobolograms and ΔE model. According to FICI interpretation, combinations of morusin with oxacillin, gentamicin, ciprofloxacin and tetracycline showed synergistic interactions (FICI = 0.13 – 0.16) against MRSA ATCC 43300 with significant reductions in antibiotic MICs (16-, 32- and 64-fold) (Table 1). The corresponding isobologram is depicted in Fig. 4A. MRSA ATCC 43300 is resistant to oxacillin and gentamicin (MIC = 64 and 256 μg/mL, respectively) while *S. epidermidis* ATCC 12228 is resistant to tetracycline (MIC = 128 μg/mL) and clindamycin (MIC = 200 μg/mL) (Aelenei et al., 2019b). In the present study, morusin reversed oxacillin resistance of MRSA ATCC 43300 by decreasing its MIC in combination to 1 μg/mL, value corresponding to susceptibility according to CLSI (2017). Morusin did not reverse gentamicin resistance of MRSA ATCC 43300 but reduced its MIC in combination 16-fold. With respect to MSSA ATCC 6538, morusin showed synergy with oxacillin, gentamicin, ciprofloxacin and tetracycline (8- to 32-fold reduction in antibiotic MICs), addition with clindamycin and indifference with erythromycin (Table 1, Fig. 4C). Morusin also acted synergistically with all antibiotics against *S. epidermidis* ATCC 12228 reversing its resistance to tetracycline (512-fold reduction of tetracycline MIC in combination) (Table 1, Fig. 4E). Antibacterial synergy of morusin in combination with amikacin and etimicin against clinical MRSA isolates has been recently reported (16- to 2- and 8- to 2-fold reduction in antibiotic MICs, respectively) (Zuo et al., 2018). Our investigations demonstrated that morusin can also act synergistically with other antibiotics (oxacillin, gentamicin, ciprofloxacin, tetracycline) and reverse oxacillin resistance of MRSA.

ΔE model confirmed all synergistic interactions (identified on the basis of FICI values) between morusin and antibiotics. For example, the three-dimensional plots of the combinations of morusin and gentamicin against MRSA ATCC 43300 are illustrated, taking into consideration both the percentage of growth (Fig. 5A) representing $E_{measured}$ and ΔE (Fig. 5B) depicting the synergism in combination (ΔE > 0). Two discrepancies between FICI interpretation and ΔE model are to be noticed. According to FICI values, combinations of morusin with erythromycin and clindamycin showed indifference and addition against MSSA ATCC 6538, respectively but they were interpreted as synergy and antagonism by ΔE model (Table 1).

Discrepancies between FICI and ΔE interpretations for the same combination have also been reported in other studies. For example, combinations of usnic acid with levofloxacin were found as indifferent by FICI model and interpreted as antagonistic by ΔE model (Segatore et al., 2012). Such discrepancies could be attributed to the particularities of each model. As mentioned before, the FICI and ΔE models are based on two prominent drug combination theories, Loewe additivity and Bliss independence, respectively (Koizumi and Iwami, 2014; Meletiadis et al., 2005; Segatore et al., 2012; Sun et al., 2008). The FICI interpretation requires the concentrations of drugs, alone and in combination, inducing the same effect whereas the ΔE model estimates the combined effects on the basis of the individual effects and compares the estimated effects with the experimental ones (Sun et al., 2008). However, a terminology reflecting the level of consistency between Loewe and Bliss models has been proposed: an interaction identified as synergistic by both models is considered "strong synergy"; in case the interaction is identified as synergistic by only one model, it is "weak synergy" (Caesar and Cech, 2019; Tang et al. 2015). As the number of drugs that are combined increases, Loewe additivity model loses accuracy whereas Bliss independence model

Table 1
Interactions between morusin and antibiotics assessed by different experimental models.

Checkerboard assay										Time-kill assay		
Atb	MIC_{Atb}*	DRI_{Atb}	MIC_{MO}*	DRI_{MO}	FICI	INT	ΔE model			Ma	$\triangle LC_{24}$***	INT
							∑SYN (n**)	∑ANT (n)	INT			
***S. aureus* ATCC 43300**												
OX	1	64	0.78	8	0.14	S	3506.05 (69)	0 (0)	S	MO	2.61 ± 0.16	S
GEN	16	16	0.39	16	0.13	S	4369.80 (60)	0 (0)	S	MO	2.15 ± 0.17	S
CIP	0.02	32	0.78	8	0.16	S	3654.80 (69)	0 (0)	S	CIP	1.18 ± 0.07	Ad
TE	1	64	0.78	8	0.14	S	3285.52 (70)	0 (0)	S	TE	1.49 ± 0.06	Ad
***S. aureus* ATCC 6538**												
OX	0.02	16	1.56	4	0.31	S	3714.51 (68)	0 (0)	S	OX	1.56 ± 0.06	Ad
ERY	0.33	1	0.10	64	1.02	I	2964.55 (62)	0 (0)	S			ND
GEN	0.02	8	1.56	4	0.38	S	4037.23 (70)	0 (0)	S	GEN	1.56 ± 0.02	Ad
CIP	0.03	16	0.78	8	0.19	S	3903.85 (70)	0 (0)	S	CIP	1.05 ± 0.03	Ad
TE	0.02	32	1.56	4	0.28	S	3271.33 (68)	0 (0)	S	TE	1.56 ± 0.32	Ad
CLI	0.01	128	3.13	2	0.51	Ad	0 (0)	−779.17 (61)	A			ND
***S. epidermidis* ATCC 12228**												
OX	0.02	16	1.56	4	0.31	S	4132.73 (63)	0 (0)	S	OX	1.80 ± 0.18	Ad
ERY	0.01	16	0.78	8	0.18	S	3882.77 (59)	0 (0)	S	ERY	1.03 ± 0.06	Ad
GEN	0.02	8	1.56	4	0.38	S	4511.68 (68)	0 (0)	S	GEN	1.24 ± 0.09	Ad
CIP	0.02	32	1.56	4	0.28	S	3953.39 (66)	0 (0)	S	CIP	1.54 ± 0.23	Ad
TE	0.25	512	1.56	4	0.25	S	4124.92 (66)	0 (0)	S	MO	1.29 ± 0.06	Ad
CLI	50	4	0.10	64	0.27	S	3575.29 (70)	0 (0)	S	MO	0.25 ± 0.07	I

Legend: A – antagonism, Ad – addition, Atb – antibiotic, CIP – ciprofloxacin, CLI – clindamycin, DRI – dose reduction index, ERY – erythromycin, FICI – fractional inhibitory concentration index (median of three FICI calculated for three independent experimental determinations), GEN – gentamicin, INT – interpretation, I – indifference, Ma – most active agent of combination, MIC – minimum inhibitory concentration, MO – morusin, ND – not determined, OX – oxacillin, S – synergism, TE – tetracycline.

* MIC in combination, μg/mL.

** n, number of combinations (amongst the 70 combinations for each strain) with statistically significant synergism or antagonism.

*** The increase in bacterial killing induced by the combination in comparison with its most active component tested alone, expressed in $\log_{10}$ CFU/mL at 24 h incubation, mean ± standard deviation.

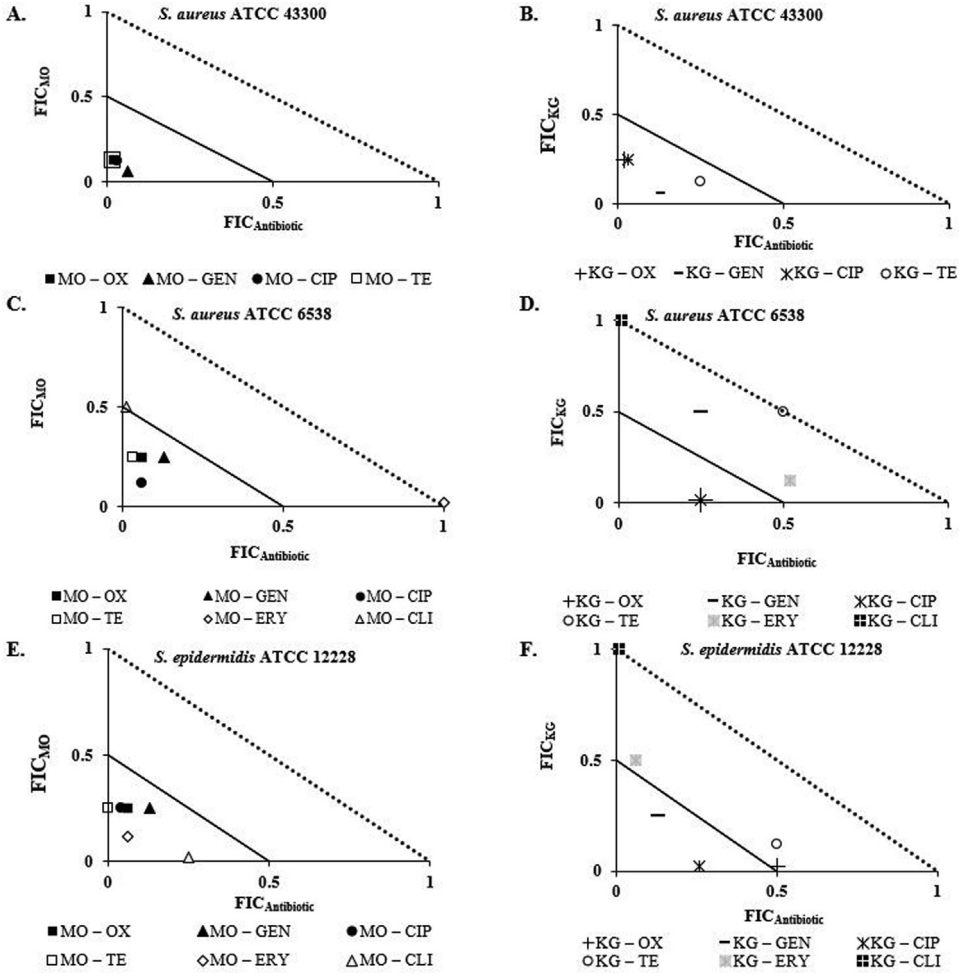

Fig. 4. Isobolograms depicting the interactions between morusin (MO) or kuwanon G (KG) and antibiotics (OX – oxacillin, CIP – ciprofloxacin, CLI – clindamycin, ERY – erythromycin, GEN – gentamicin, TE – tetracycline) against *S. aureus* ATCC 43300 (MRSA) (A, B), *S. aureus* ATCC 6538 (MSSA) (C, D) and *S. epidermidis* ATCC 12228 (E, F).

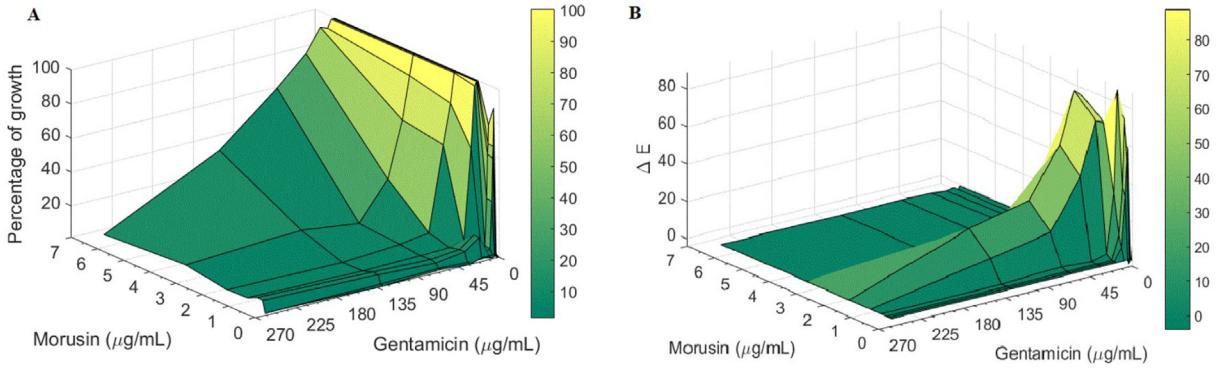

Fig. 5. Three-dimensional plot of the experimental percentage of growth between morusin and gentamicin against *S. aureus* ATCC 43300 (MRSA) (A). Three-dimensional plot of the difference between the predicted and experimental percentage of growth between morusin and gentamicin against *S. aureus* ATCC 43300 (MRSA) (△E model) (B).

maintains its predictability (Caesar and Cech 2019; Lederer et al. 2019).

In contrast to checkerboard method which assesses bacteriostatic synergism, time-kill assay evaluates bactericidal synergism (Zuo et al., 2016). Time-killing experiments were performed at sub-inhibitory concentrations (½ × MIC) for all the combinations showing synergy in the checkerboard assay. The kinetic of the interaction between bacterial cells and antibacterial agents was followed for 48 h, the change in bacterial killing induced by a combination in comparison with its most active component being determined at 24 h ($\triangle LC_{24}$). Bactericidal synergism ($\triangle LC_{24} \geq 2$ $\log_{10}$ CFU/mL) was detected only for the combinations of morusin with gentamicin and oxacillin against MRSA ATCC 43300; these combinations caused 2.61 and 2.15 $\log_{10}$ decrease in colony counts, respectively, in comparison with the most active component of the combination tested alone (morusin). Eleven combinations showed additive kinetics ($\triangle LC_{24}$ = 1.03–1.80 $\log_{10}$ CFU/mL) and one combination was found indifferent ($\triangle LC_{24}$ = 0.25 $\log_{10}$ CFU/mL). Combinations showing additive kinetics are also of interest as they display more potent bactericidal effects than the most active com-

ponent of the combination tested alone (Table 1). Only the time-kill curves corresponding to the combinations showing bactericidal synergism were represented graphically in Fig. 6.

The partial agreement (44 – 88%) between the checkerboard and time-kill tests, reported in many studies, could be explained, in large part, by the different processes assessed in these two tests: inhibition of bacterial growth in the former and bacterial killing in the latter (White et al., 1996). For example, morusinol, a prenylflavonoid in white mulberry root bark, showed synergistic interactions with amikacin against clinical MRSA isolates in the checkerboard assay (FICI = 0.09 – 0.50) but in the time-kill experiments, the combinations of morusinol with amikacin (at MIC) were indifferent (Zuo et al., 2018).

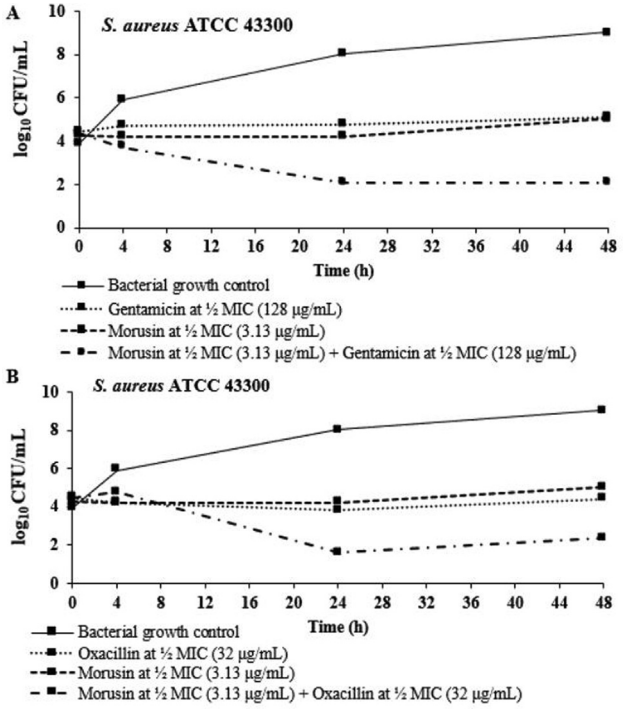

Fig. 6. Time-kill curves of morusin, gentamicin and oxacillin (each at ½ × MIC) alone and in combination against *S. aureus* ATCC 43300 (MRSA).

In accordance with FICI interpretation, kuwanon G showed synergy with oxacillin, gentamicin, ciprofloxacin and tetracycline against MRSA ATCC 43300 (64-, 8-, 32- and 4-fold reduction in antibiotic MICs, respectively) and reversed its resistance to oxacillin (Table 2, Fig. 4B). Synergistic interactions were also found for the combinations of kuwanon G with oxacillin against MSSA ATCC 6538 and kuwanon G with gentamicin against *S. epidermidis* ATCC 12228; combinations of kuwanon G with ciprofloxacin showed synergy against both strains. In these combinations, antibiotic MIC was lowered 4- and 8-fold (Table 2, Fig. 4D,F). Furthermore, six additive interactions were detected showing 2-, 4- and 16-fold decrease in antibiotic MICs against MSSA ATCC 6538 and *S. epidermidis* ATCC 12228 (Table 2, Fig. 4D,F). ΔE model confirmed synergy for six of eight combinations described as synergistic using FICI interpretation (Table 2). Similar to morusin, time-killing experiments were performed (at ½ × MIC) for all the synergistic combinations in the checkerboard assay but no bactericidal synergy was detected. It is worth mentioning that the combination of kuwanon G with ciprofloxacin showed additive bactericidal effects on MRSA ATCC 43300 and *S. epidermidis* ATCC 12228 ($\triangle LC_{24}$ = 1.72 and 1.56 $\log_{10}$ CFU/mL, respectively). Combination of kuwanon G with oxacillin showed weak additive effect on MRSA ATCC 43300 ($\triangle LC_{24}$ = 1.08 $\log_{10}$ CFU/mL). Other six combinations were found to be indifferent ($\triangle LC_{24}$ = 0.18 – 0.90 $\log_{10}$ CFU/mL) (Table 2).

Overall, our investigations clearly indicate that morusin and kuwanon G, prenylated phenolics in *Morus* species, enhance the antibacterial potency of several commonly used antibiotics against MSSA, MRSA and *S. epidermidis*. The alteration of bacterial membrane integrity undoubtedly plays a major role in antibiotic enhancing effects as it potentiates the activity of membrane targeting antibiotics (oxacillin) and facilitates the penetration and

Table 2
Interactions between kuwanon G and antibiotics assessed by different experimental models.

Checkerboard assay										Time-kill assay		
Atb	MIC_{Atb}*	DRI_{Atb}	MIC_{KG}*	DRI_{KG}	FICI	INT	ΔE model			Ma	$\triangle LC_{24}$***	INT
							∑SYN (n**)	∑ANT (n)	INT			
***S. aureus* ATCC 43300**												
OX	1	64	3.13	4	0.27	S	442.20 (47)	0 (0)	S	KG	1.08 ± 0.01	Ad
GEN	32	8	0.78	16	0.19	S	0 (0)	0 (0)	I	KG	0.77 ± 0.05	I
CIP	0.02	32	3.13	4	0.38	S	3385.19 (69)	0 (0)	S	CIP	1.72 ± 0.03	Ad
TE	0.25	4	1.56	8	0.38	S	1492.86 (37)	0 (0)	S	KG	0.18 ± 0.03	I
***S. aureus* ATCC 6538**												
OX	0.06	4	0.20	64	0.27	S	0 (0)	−328.7 (31)	A	OX	0.67 ± 0.06	I
ERY	0.17	2	1.56	8	0.63	Ad	0 (0)	0 (0)	I			ND
GEN	0.03	4	12.50	2	0.75	Ad	1526 (36)	0 (0)	S			ND
CIP	0.13	4	0.20	64	0.27	S	3442.77 (59)	0 (0)	S	CIP	0.56 ± 0.09	I
TE	0.25	2	12.50	2	1	Ad	1416.67 (18)	0 (0)	S			ND
CLI	0.01	128	12.50	1	1.01	I	3575.29 (70)	0 (0)	S	KG	0.52 ± 0.03	I
***S. epidermidis* ATCC 12228**												
OX	0.13	2	0.20	64	0.52	Ad	0 (0)	−10.74 (2)	I			ND
ERY	0.01	16	6.25	2	0.56	Ad	81.33 (19)	0 (0)	I			ND
GEN	0.02	8	3.13	4	0.38	S	2284 (57)	0 (0)	S	GEN	0.90 ± 0.07	I
CIP	0.13	4	0.20	64	0.28	S	3547.84 (59)	0 (0)	S	CIP	1.56 ± 0.06	Ad
TE	64	2	1.56	8	0.62	Ad	2455 (24)	0 (0)	S			ND
CLI	1	200	12.50	1	1.01	I	5.30 (5)	0 (0)	I	KG	0.23 ± 0.08	I

Legend: A – antagonism, Ad – addition, Atb – antibiotic, CIP – ciprofloxacin, CLI – clindamycin, DRI – dose reduction index, ERY – erythromycin, FICI – fractional inhibitory concentration index (median of three FICI calculated for three independent experimental determinations), GEN – gentamicin, INT – interpretation, I – indifference, KG – kuwanon G, Ma – most active agent of combination, MIC – minimum inhibitory concentration, ND – not determined, OX – oxacillin, S – synergism, TE – tetracycline.

* MIC in combination, µg/mL.

** n, number of combinations (amongst the 70 combinations for each strain) with statistically significant synergism or antagonism.

*** The increase in bacterial killing induced by the combination in comparison with its most active component tested alone, expressed in $\log_{10}$ CFU/mL at 24 h incubation, mean ± standard deviation.

activity of antibiotics inside the bacterial cell (ciprofloxacin, erythromycin, gentamicin, tetracycline, clindamycin). It is worth mentioning that the doses of morusin and kuwanon G in the combinations reported as synergistic by FICI and ΔE models (morusin: ≤ 1.56 μg/mL equiv. to 3.71 μM; kuwanon G: ≤ 3.13 μg/mL equiv. to 4.52 μM) are lower than the ones found to be cytotoxic in human normal cells (morusin: IC_{50} = 9.48 μg/mL in human normal mammary epithelial cells (MCF-10A), IC_{50} = 12.45 μg/mL in human normal liver cells (LO2), no alteration in viability of HaCaT keratinocytes and MC/9 mast cells at concentrations of up to 5 μM; kuwanon G: no alteration in viability of HaCaT keratinocytes and MC/9 mast cells at concentrations up to 20 and 10 μM, respectively) (Gao et al., 2017; Jin et al., 2019; Li et al., 2015). Unfortunately, the isolation of pure phytochemicals from plant material is a complex, time-consuming, costly and low-yield process. Chemical synthesis is an alternative approach to produce phytochemicals in higher yields with lower costs (Zhou et al., 2011). Morusin has already been synthesized from phloroglucinol (Tseng et al., 2010). To the best of our knowledge, the synthesis of kuwanon G has not been reported yet but other natural Diels – Alder type adducts (kuwanons I and J, panduratin A, nicolaioidesin C) have been successfully obtained by chemical synthesis based on biosynthesis models (biomimetic synthesis) (Nasir et al., 2017).

4. Conclusions

The present study investigated the ability of morusin and kuwanon G to potentiate the effects of some common antibiotics against MSSA, MRSA and *S. epidermidis*. Twenty combinations (14 morusin-antibiotic combinations, six kuwanon G-antibiotic combinations) showed bacteriostatic synergy according to both FICI and ΔE models. In these combinations, morusin and kuwanon G had strong impact on antibiotic MICs reducing their values 4- to 512-fold. Both prenylated compounds reversed oxacillin resistance of MRSA. In addition, morusin reversed tetracycline resistance of *S. epidermidis*. Combination of sub-inhibitory concentrations (½ × MIC) of morusin and oxacillin or morusin and gentamicin displayed bactericidal synergy against MRSA. Alteration of bacterial membrane is responsible, at least in part, for the increase in antibiotic susceptibility and reversal of antibiotic resistance. To conclude, our findings support that both morusin and kuwanon G are good candidates for the development of novel antibacterial combination therapies. Further studies are necessary to confirm the *in vivo* efficacy of these combinations.

Funding

This research did not receive any specific grant from funding agencies in the public, commercial, or not-for-profit sectors.

Declaration of Competing Interest

The authors declare no conflict of interest.

Appendix A. Supplementary material

Supplementary data to this article can be found online at https://doi.org/10.1016/j.jsps.2020.08.006.

References

Abbas, G.M., Abdel Bar, F.M., Baraka, H.N., Gohar, A.A., Lahloub, M.F., 2014. A new antioxidant stilbene and other constituents from the stem bark of *Morus nigra* L. Nat. Prod. Res. 28 (13), 952–959. https://doi.org/10.1080/14786419.2014.900770.

Aelenei, P., Miron, A., Trifan, A., Bujor, A., Gille, E., Aprotosoaie, A.C., 2016. Essential oils and their components as modulators of antibiotic activity against Gram-negative bacteria. Medicines 3 (3), 19. https://doi.org/10.3390/medicines3030019.

Aelenei, P., Luca, S.V., Horhogea, C.E., Rimbu, C.M., Dimitriu, G., Macovei, I., Silion, M., Aprotosoaie, A.C., Miron, A., 2019a. *Morus alba* leaf extract: Metabolite profiling and interactions with antibiotics against *Staphylococcus* spp. including MRSA. Phytochem. Lett. 31, 217–224. https://doi.org/10.1016/j.phytol.2019.04.006.

Aelenei, P., Rimbu, C.M., Guguianu, E., Dimitriu, G., Aprotosoaie, A.C., Brebu, M., Horhogea, C.E., Miron, A., 2019b. Coriander essential oil and linalool – interactions with antibiotics against Gram-positive and Gram-negative bacteria. Lett. Appl. Microbiol. 68 (2), 156–164. https://doi.org/10.1111/lam.13100.

Alikhani, A., Salehifar, E., 2012. An unreported clindamycin adverse reaction: wrist monoarthritis. Iran J. Pharm. Res. 11 (3), 959–962 https://www.ncbi.nlm.nih.gov/pmc/articles/PMC3813142/.

Aquino, A., Chan, J., Giolma, K., Loh, M., 2010. The effect of a fullerene water suspension on the growth, cell viability, and membrane integrity of *Escherichia coli* B23. J. Exp. Microbiol. Immunol. 14, 13–20 https://www.semanticscholar.org/paper/The-Effect-of-a-Fullerene-Water-Suspension-on-the-Aquino-Chan/c4093d67a6988882d0bee5f04b237e2a1705837c.

Araya-Cloutier, C., 2017. Antibacterial prenylated isoflavonoids and stilbenoids. Quantitative structure-activity relationships and mode of action PhD Thesis. Wageningen University, the Netherlands.

Araya-Cloutier, C., Vincken, J.P., van Ederen, R., den Besten, H.M.W., Gruppen, H., 2018. Rapid membrane permeabilization of *Listeria monocytogenes* and *Escherichia coli* induced by antibacterial prenylated phenolic compounds from legumes. Food Chem. 240, 147–155. https://doi.org/10.1016/j.foodchem.2017.07.074.

Bassolé, I.H.N., Juliani, H.R., 2012. Essential oils in combination and their antimicrobial properties. Molecules 17 (4), 3989–4006. https://doi.org/10.3390/molecules17043989.

Basri, D.F., Jaffar, N., Zin, N.M., Santhana Raj, L., 2013. Electron microscope study of gall extract from *Quercus infectoria* in combination with vancomycin against MRSA using post-antibiotic effect determination. Int. J. Pharmacol. 9 (2), 150–156 https://scialert.net/abstract/?doi=ijp.2013.150.156.

Bocquet, L., Sahpaz, S., Bonneau, N., Beaufay, C., Mahieux, S., Samaillie, J., Roumy, V., Jacquin, J., Bordage, S., Hennebelle, T., Chai, F., Quetin-Leclercq, J., Neut, C., Rivière, C., 2019. Phenolic compounds from *Humulus lupulus* as natural antimicrobial products: new weapons in the fight against methicillin resistant *Staphylococcus aureus*, *Leishmania mexicana* and *Trypanosoma brucei* strains. Molecules 24, 1024. https://doi.org/10.3390/molecules24061024.

Caesar, L.K., Cech, N.B., 2019. Synergy and antagonism in natural product extracts: when 1 + 1 does not equal 2. Nat. Prod. Rep. 36 (6), 869–888. https://doi.org/10.1039/C9NP00011A.

Chan, B.C.L., Ip, M., Gong, H., Lui, S.L., See, R.H., Jolivalt, C., Fung, K.P., Leung, P.C., Reiner, N.E., Lau, C.B.S., 2013. Synergistic effects of diosmetin with erythromycin against ABC transporter over-expressed methicillin-resistant *Staphylococcus aureus* (MRSA) RN4220/pUL5054 and inhibition of MRSA pyruvate kinase. Phytomedicine 20 (7), 611–614. https://doi.org/10.1016/j.phymed.2013.02.007.

Choo, E.J., Chambers, H.F., 2016. Treatment of methicillin-resistant *Staphylococcus aureus* bacteremia. Infect. Chemother. 48 (4), 267–273. https://doi.org/10.3947/ic.2016.48.4.267.

Clinical and Laboratory Standards Institute (CLSI), 2017. Performance Standards for Antimicrobial Susceptibility Testing, 27th ed., CLSI supplement M100, Wayne, PA.

Cunha, B.A., 2001. Antibiotic side effects. Med. Clin. North Am. 85 (1), 149–185. https://doi.org/10.1016/S0025-7125(05)70309-6.

Eladli, M.G., Alharbi, N.S., Khaled, J.M., Kadaikunnan, S., Alobaidi, A.S., Alyahya, S.A., 2019. Antibiotic-resistant *Staphylococcus epidermidis* isolated from patients and healthy students comparing with antibiotic-resistant bacteria isolated from pasteurized milk. Saudi J. Biol. Sci. 26, 1285–1290. https://doi.org/10.1016/j.sjbs.2018.05.008.

Gao, L., Wang, L., Sun, Z., Li, H., Wang, Q., Yi, C., Wang, X., 2017. Morusin shows potent antitumor activity for human hepatocellular carcinoma *in vitro* and *in vivo* through apoptosis induction and angiogenesis inhibition. Drug Des. Devel. Ther. 11, 1789–1802. https://doi.org/10.2147/DDDT.S138320.

Guo, H., Xu, Y., Huang, W., Zhou, H., Zheng, Z., Zhao, Y., He, B., Zhu, T., Tang, S., Zhu, Q., 2016. Kuwanon G preserves LPS-induced disruption of gut epithelial barrier *in vitro*. Molecules 21 (11), 1597. https://doi.org/10.3390/molecules21111597.

Hendry, E.R., Worthington, T., Conway, B.R., Lambert, P.A., 2009. Antimicrobial efficacy of eucalyptus oil and 1,8-cineole alone and in combination with chlorhexidine digluconate against microorganisms growing in planktonic and biofilm cultures. J. Antimicrob. Chemother. 64 (6), 1219–1225. https://doi.org/10.1093/jac/dkp362.

Hosseini, A.-S., Akramian, M., Khadivi, A., Salehi-Arjmand, H., 2018. Phenotypic and chemical variation of black mulberry (*Morus nigra*) genotypes. Ind. Crops Prod. 117, 260–271. https://doi.org/10.1016/j.indcrop.2018.03.007.

Jin, S.E., Ha, H., Shin, H.-K., Seo, C.-S., 2019. Anti-allergic and anti-inflammatory effects of kuwanon G and morusin on MC/9 mast cells and HaCaT keratinocytes. Molecules 24 (2), 265. https://doi.org/10.3390/molecules24020265.

Kirchhoff, C., Cypionka, H., 2017. Propidium ion enters viable cells with high membrane potential during live-dead staining. J. Microbiol. Methods 142, 79–82. https://doi.org/10.1016/j.mimet.2017.09.011.

Kohanski, M.A., Dwyer, D.J., Collins, J.J., 2010. How antibiotics kill bacteria: from targets to networks. Nat. Rev. Microbiol. 8 (6), 423–435. https://doi.org/10.1038/nrmicro2333.

Koizumi, Y., Iwami, S., 2014. Mathematical modeling of multi-drugs therapy: a challenge for determining the optimal combinations of antiviral drugs. Theor. Biol. Med. Model 11, 41. https://doi.org/10.1186/1742-4682-11-41.

Lederer, S., Dijkstra, T.M.H., Heskes, T., 2019. Additive dose response models: defining synergy. Front. Pharmacol. 10, 1384. https://doi.org/10.3389/fphar.2019.01384.

Lee, Y.-S., Kang, O.-H., Choi, J.-G., Oh, Y.-C., Chae, H.-S., Kim, J.K., Park, H., Sohn, D.H., Wang, Z.-T., Kwon, D.-Y., 2008. Synergistic effects of the combination of galangin with gentamicin against methicillin-resistant *Staphylococcus aureus*. J. Microbiol. 46 (3), 283–288. https://doi.org/10.1007/s12275-008-0012-7.

Lee, G.S., Kim, E.S., Cho, S.I., Kim, J.H., Choi, G., Ju, Y.S., Park, S.H., Jeong, S.I.I., Kim, H.J., 2010. Antibacterial and synergistic activity of prenylated chalcone isolated from the roots of *Sophora flavescens*. Korean Soc. Appl. Biol. Chem. 53, 290–296. https://doi.org/10.3839/jksabc.2010.045.

Lee Ventola, C., 2015. The antibiotic resistance crisis. Part I: causes and threats. P T. 40 (4), 277–283.

Li, H., Wang, Q., Dong, L., Liu, C., Sun, Z., Gao, L., Wang, X., 2015. Morusin suppresses breast cancer cell growth *in vitro* and *in vivo* through C/EBPβ and PPARγ mediated lipoapoptosis. J. Exp. Clin. Cancer Res. 34, 137. https://doi.org/10.1186/s13046-015-0252-4.

Mazimba, O., Majinda, R.R.T., Motlhanka, D., 2011. Antioxidant and antibacterial constituents from *Morus nigra*. Afr. J. Pharm. Pharmacol. 5 (6), 751–754. https://doi.org/10.5897/AJPP11.260.

Meletiadis, J., Verweij, P.E., TeDorsthorst, D.T., Meis, J.F., Mouton, J.W., 2005. Assessing *in vitro* combinations of antifungal drugs against yeasts and filamentous fungi: comparison of different drug interaction models. Med. Mycol. 43 (2), 133–152. https://doi.org/10.1080/13693780410001731547.

Mulyaningsih, S., Sporer, F., Zimmermann, S., Reichling, J., Wink, M., 2010. Synergistic properties of the terpenoids aromadendrene and 1,8-cineole from the essential oil of *Eucalyptus globulus* against antibiotic-susceptible and antibiotic-resistant pathogens. Phytomedicine 17 (13), 1061–1066. https://doi.org/10.1016/j.phymed.2010.06.018.

Nasir, S.B., Tee, J.T., Rahman, N.A., Chee, C.F., 2017. Biosynthesis and biomimetic synthesis of flavonoid Diels – Alder natural products, in: Justino, G. (Ed.), Flavonoids – from biosynthesis to human health. IntechOpen, pp. 167-188. http://dx.doi.org/10.5772/intechopen.68781.

Otto, M., 2009. *Staphylococcus epidermidis* – the "accidental" pathogen. Nat. Rev. Microbiol. 7 (8), 555–567. https://doi.org/10.1038/nrmicro2182.

Otto, R.G., van Gorp, E., Kloezen, W., Meletiadis, J., van den Berg, S., Mouton, J.W., 2019. An alternative strategy for combination therapy: Interactions between polymyxin B and non-antibiotics. Int. J. Antimicrob. Agents 53 (1), 34–39. https://doi.org/10.1016/j.ijantimicag.2018.09.003.

Pang, D., Liao, S., Wang, W., Mu, L., Li, E., Shen, W., Liu, F., Zou, Y., 2019. Destruction of the cell membrane and inhibition of cell phosphatidic acid biosynthesis in *Staphylococcus aureus*: an explanation for the antibacterial mechanism of morusin. Food & Funct. 10, 6438–6446. https://doi.org/10.1039/C9FO01233H.

Park, K.M., You, J.S., Lee, H.Y., Baek, N.I., Hwang, J.K., 2003. Kuwanon G: an antibacterial agent from the root bark of *Morus alba* against oral pathogens. J. Ethnopharmacol. 84 (2–3), 181–185. https://doi.org/10.1016/S0378-8741(02)00318-5.

Rüegg, T., Calderón, A.I., Queiroz, E.F., Solis, P.N., Marston, A., Rivas, F., Ortega-Barría, E., Hostettmann, K., Gupta, M.P., 2006. 3-Farnesyl-2-hydroxybenzoic acid is a new anti-*Helicobacter pylori* compound from *Piper multiplinervium*. J. Ethnopharmacol. 103 (3), 461–467. https://doi.org/10.1016/j.jep.2005.09.014.

Sakagami, Y., Iinuma, M., Piyasena, K.G.N.P., Dharmaratne, H.R.W., 2005. Antibacterial activity of α-mangostin against vancomycin resistant *Enterococci* (VRE) and synergism with antibiotics. Phytomedicine 12 (3), 203–208. https://doi.org/10.1016/j.phymed.2003.09.012.

Seesom, W., Jaratrungtawee, A., Suksamrarn, S., Mekseepralard, C., Ratananukul, P., Sukhumsirichart, W., 2013. Antileptospiral activity of xanthones from *Garcinia mangostana* and synergy of gamma-mangostin with penicillin G. BMC Complement. Altern. Med. 13, 182. https://doi.org/10.1186/1472-6882-13-182.

Segatore, B., Bellio, P., Setacci, D., Brisdelli, F., Piovano, M., Garbarino, J.A., Nicoletti, M., Amicosante, G., Perilli, M., Celenza, G., 2012. *In vitro* interaction of usnic acid in combination with antimicrobial agents against methicillin-resistant *Staphylococcus aureus* clinical isolates determined by FICI and ΔE model methods. Phytomedicine 19 (3–4), 341–347. https://doi.org/10.1016/j.phymed.2011.10.012.

Sohn, H.Y., Son, K.H., Kwon, C.S., Kwon, G.S., Kang, S.S., 2004. Antimicrobial and cytotoxic activity of 18 prenylated flavonoids isolated from medicinal plants: *Morus alba* L., *Morus mongolica* Schneider, *Broussnetia papyrifera* (L.) Vent, *Sophora flavescens* Ait and *Echinosophora koreensis* Nakai. Phytomedicine 11 (7–8), 666–672. https://doi.org/10.1016/j.phymed.2003.09.005.

Subramani, R., Narayanasamy, M., Feussner, K.-D., 2017. Plant-derived antimicrobials to fight against multi-drug-resistant human pathogens. 3 Biotech. 7, 172. https://doi.org/10.1007/s13205-017-0848-9.

Sun, S., Li, Y., Guo, Q., Shi, C., Yu, J., Ma, L., 2008. *In vitro* interactions between tacrolimus and azoles against *Candida albicans* determined by different methods. Antimicrob. Agents Chemother. 52 (2), 409–417. https://doi.org/10.1128/AAC.01070-07.

Tanaka, H., Atsumi, I., Shirota, O., Sekita, S., Sakai, E., Sato, M., Murata, J., Murata, H., Darnaedi, D., Chen, I.S., 2011. Three new constituents from the roots of *Erythrina variegata* and their antibacterial activity against methicillin-resistant *Staphylococcus aureus*. Chem. Biodivers. 8 (3), 476–482. https://doi.org/10.1002/cbdv.201000068.

Tang, J., Wennerberg, K., Aittokallio, T., 2015. What is synergy? The Saariselkä agreement revisited. Front. Pharmacol. 6, 181. https://doi.org/10.3389/fphar.2015.00181.

Tseng, T.-H., Chuang, S.-K., Hu, C.-C., Chang, C.-F., Huang, Y.-C., Lin, C.-W., Lee, Y.-J., 2010. The synthesis of morusin as a potent antitumor agent. Tetrahedron 66 (6), 1335–1340. https://doi.org/10.1016/j.tet.2009.12.002.

Turan, I., Demir, S., Kilinc, K., Burnaz, N.A., Yaman, S.O., Akbulut, K., Mentese, A., Aliyazicioglu, Y., Deger, O., 2017. Antiproliferative and apoptotic effect of *Morus nigra* extract on human prostate cancer cells. Saudi Pharm. J. 25, 241–248. https://doi.org/10.1016/j.jsps.2016.06.002.

van Vuuren, S., Viljoen, A., 2011. Plant-based antimicrobial studies – methods and approaches to study the interaction between natural products. Planta Med. 77 (11), 1168–1182. https://doi.org/10.1055/s-0030-1250736.

Vijayan, K., Tikader, A., Weiguo, Z., Nair, C.V., Ercisli, S., Tsou, C.-H., 2011. Morus. In: Kole, C. (Ed.), Wild Crop Relatives: Genomic and Breeding Resources, Tropical and Subtropical Fruits. Springer-Verlag, Berlin Heidelberg, pp. 75–95 https://www.researchgate.net/publication/251406104_Morus.

Wesołowska, O., Gasiorowska, J., Petrus, J., Czarnik-Matusewicz, B., Michalak, K., 2014. Interaction of prenylated chalcones and flavanones from common hop with phosphatidylcholine model membranes. BBA, 173–184. https://doi.org/10.1016/j.bbamem.2013.09.009. 1838 (1 Pt B).

White, R.L., Burgess, D.S., Manduru, M., Bosso, J.A., 1996. Comparison of three different *in vitro* methods of detecting synergy: time-kill, checkerboard, and E test. Antimicrob. Agents Chemother. 40 (8), 1914–1918 https://aac.asm.org/content/40/8/1914.

Wu, S.-C., Han, F., Song, M.-R., Chen, S., Li, Q., Zhang, Q., Zhu, K., Shen, J.-Z., 2019. Natural flavones from *Morus alba* against methicillin-resistant *Staphylococcus aureus* via targeting the proton motive force and membrane permeability. J. Agric. Food Chem. 67, 10222–10234. https://doi.org/10.1021/acs.jafc.9b01795.

Zacchino, S.A., Butassi, E., Di Liberto, M., Raimondi, M., Postigo, A., Sortino, M., 2017. Plant phenolics and terpenoids as adjuvants of antibacterial and antifungal drugs. Phytomedicine 37, 27–48. https://doi.org/10.1016/j.phymed.2017.10.018.

Zhang, D.-Y., Wan, Y., Hao, J.-Y., Hu, R.-Z., Chen, C., Yao, X.-H., Zhao, W.-G., Liu, Z.-Y., Li, L., 2018. Evaluation of the alkaloid, polyphenols, and antioxidant contents of various mulberry cultivars from different planting areas in eastern China. Ind. Crops Prod. 122, 298–307. https://doi.org/10.1016/j.indcrop.2018.05.065.

Zhou, X., Jia, F., Liu, X., Yang, J., Zhang, Y., Wang, Y., 2011. *In vitro* synergistic interaction of 5-*O*-methylglovanon and ampicillin against ampicillin resistant *Staphylococcus aureus* and *Staphylococcus epidermidis* isolates. Arch. Pharm. Res. 34 (10), 1751–1757. https://doi.org/10.1007/s12272-011-1019-x.

Zuo, G.Y., Wang, C.J., Han, J., Li, Y.Q., Wang, G.C., 2016. Synergism of coumarins from the Chinese drug *Zanthoxylum nitidum* with antibacterial agents against methicillin-resistant *Staphylococcus aureus* (MRSA). Phytomedicine 23 (14), 1814–1820. https://doi.org/10.1016/j.phymed.2016.11.001.

Zuo, G.Y., Yang, C.X., Han, J., Li, Y.Q., Wang, G.C., 2018. Synergism of prenylflavonoids from *Morus alba* root bark against clinical MRSA isolates. Phytomedicine 39, 93–99. https://doi.org/10.1016/j.phymed.2017.12.023.